The Influence of Plastic-Strain-Induced Anisotropy Modeled as Combined Isotropic-Kinematic Hardening in the Tension-Torsion Straining Problem (I)

— Representation of the Back Stress and Applicability of the Combined Isotropic-Kinematic Hardening Model —

Yeong Sung Suh*

(*Received August 2, 1997*)

In order to express the plastic-strain-induced anisotropy at finite deformation of ductile metals, a combined isotropic-kinematic hardening model which is a particular form of anisotropic hardening, is an appropriate model because of its simple and convenient mathematical formulation. This paper examines the applicability of the model in the computation of general straining problems by performing a numerical tension-torsion test. The anisotropy generated by plastic flow is expressed by back stress. The evolution equation contains form-invariant isotropic functions of plastic strain rate and back stress and also involves the spin associated with induced anisotropy. A numerical fitting procedure allowed us to show that circles modeled as combined isotropic-kinematic hardening around the loading nose are in good agreement with the experimental yield loci taken from the nonproportional straining. The measure of checking the applicability of combined isotropic-kinematic hardening by analyzing the total stress history has also been demonstrated by simulating an extrusion process using the finite-element method. From the computed results, the angle variations between the principal stress direction and the material direction, initially axial, were observed if they are small enough in the active plastic deformation region to ensure that the stress point will move along the part of the yield locus exhibiting nearly uniform curvature. This indicated that stress and deformation can be predicted with combined isotropic-kinematic hardening as long as the loading is not reversed.

Key Words: Plastic-Strain-Induced Anisotropy, Combined Isotropic-Kinematic Hardening, Yield Locus, Tension-Torsion, Back Stress, Least Square Fit, Extrusion

1. Introduction

Extensive experimental evidence has indicated that materials exhibit significant anisotropic hardening induced by plastic deformation. Subsequent yield surfaces, which expand and translate in stress space, are also subject to shape changes. These are more evident at large deformation. In this context, it is important to develop satisfactory elastic-plastic constitutive relations to express the influence of plastic-strain-induced anisotropy at finite deformation, since virtually all ductile metals exhibit this characteristic.

The elastic-plastic constitutive relations must incorporate the influence of the various components of plastic-strain-induced anisotropy, such as the self-equilibrating internal stresses caused by dislocation pile-up at imperfections, or inclusions in crystallites or at grain boundaries of polycrystalline metals, or with residual-type stresses generated in the crystallites of a polycrystalline metal due to mismatch plastic strains in the

* Department of Mechanical Engineering, Hannam University, 133 Ojung-dong, Taeduk-gu, Taejon, Korea, 306-791

variously oriented grains. These can be modeled by the back stress, a second order tensor internal variable which represents the kinematic shift of the yield surface. Another component of the induced anisotropy is associated with the differential hardening of various slip systems and texture evolution which are partly responsible for the shape change of the yield surface. Since the micromechanisms which generate them are embedded in the material, the evolution laws for the internal variables which are used to model such mechanisms must reflect the influence of both deformation and rotation. Several workers presented different descriptions of distortional hardening (Kurtyka and Zyczkowski, 1985, 1996 ; Mazilu and Meyers, 1985, Gupta and Meyers, 1986, 1992 ; Helling and Miller, 1987 ; Voyiadjis and Foroozesh, 1990), but most of them focus on the fitting of the distorted yield loci rather than providing an evolution model for numerical prediction of material deformation. In this paper, rather than taking account of the distortion of yield loci, which is a complete description of the geometry, only the expansion and the translation of the yield surface were considered based on combined isotropic -kinematic hardening associated with von Mises yield surface, which is much more practical and easier for implementation in a numerical scheme. Experiments carried out by Helling *et al.* (1986) indicate that for smooth changes of the strain vector, the subsequent yield surface maintains an effectively circular nose geometry, which can be analytically expressed as a combined isotropic -kinematic hardening with von Mises yield criterion in the axial stress - generalized shear stress space. In the major deformation regions of most metal-forming processes, drastic changes in the ratios of the strain rate vector components are not likely to occur. This suggests that in many metal -forming processes, the stress point remains in the neighborhood of the nose of the yield surface. This simplifies the selection of an accurate constitutive relation such that stress analysis can be associated with combined isotropic-kinematic hardening, which can represent expansion and translation of the varying yield surface.

Modeling strain- or deformation-induced anisotropy has long been a subject of interest among researchers (Loret, 1983 ; Dafalias, 1983, 1985a, b ; Zbib and Aifantis, 1987, 1988a, b ; Paulun and Pecherski, 1985, 1987 ; Van Der Giessen *et al*, 1992, Kuroda, 1995) since Mandel (1978) set up a framework for a relevant constitutive theory. Most of the works have adopted the concept of plastic spin appearing in Mandel's framework to describe strain-induced anisotropy. In more recent work, Ning and Aifantis (1997) described deformation induced anisotropy in polycrystalline solids at both the grain and a aggregate levels. They have demonstrated deformation induced anisotropy by adopting a scale -invariant approach and compared their theoretical predictions with combined tension-torsion data. These works can be regarded to phenomenological approaches. Among the continuum approaches, an elastic-plastic theory which takes account of the spin associated with plastic-strain-induced anisotropy through a combined isotropic-kinematic hardening model has been proposed by Agah-Tehrani *et al.* (1987). This theory, which is based on the multiplicative decomposition of the deformation gradient into a plastic followed by an elastic deformation, utilizes the representation theorems for symmetric and anti-symmetric second order tensors to present a general isotropic or form-invariant function in terms of certain basic functions. The resulting isotropic function of the back stress expresses the direct effect of the rate of strain and the influence of the rotation associated with the straining of lines of material elements which carry the embedded back stress. Although the importance of all the tensorial base functions utilized in the evolution law for the back stress is as yet undetermined, Lee and Agah-Tehrani (1988) and Suh *et al.* (1991) have demonstrated that incorporating the base functions in a simplified form representative of the influence of such a rotation term is of major importance in the stress analysis of nonproportional, homogeneous and nonhomogeneous straining problems. It was also shown in these papers that inclusion of this rotation term eliminated the oscillation of the stress-strain

curve in shear at large strains, which was erroneously predicted during the simple shearing of a rectangular block (Nagtegaal and de Jong, 1982).

In this paper, the basic theory of the evolution model for plastic-strain-induced anisotropy is briefly demonstrated, and the representation of the back stress in the deviatoric stress space is presented. The applicability of the combined isotropic-kinematic hardening is then examined by fitting the yield loci obtained from the tension-torsion experimental data provided from Cheng and Krempl (1989). Finally, an extrusion problem is simulated by the finite-element method in order to introduce a means of checking that the loading stress remains in the neighborhood of the nose of the yield surface during forming.

2. Structure of Back Stress Evolution Involving Plastic-Strain-Induced Anisotropy

As plastic strain increases, the plastic-strain-induced anisotropy becomes more significant. The micro-mechanisms which generate the plastic-strain-induced anisotropy are embedded in the material and are convected in both translation and rotation with the changing deformation (Lee, 1985). The Bauschinger effect is modeled by introducing the back stress α, a second-order tensor internal variable. Physically the back stress α is a residual stress field embedded in the polycrystalline material at the crystallite or crystal-lattice level due to deformation of the agglomeration of the anisotropic crystallites and to dislocation pile-ups in the crystallites. This back stress α affects the magnitude of the superimposed applied stress needed to produce additional plastic flow and thus produces the Bauschinger effect. A complete analysis of the rotation and variation of the back stress α calls for a micromechanical analysis of the generation of residual stress in the crystallites of the polycrystalline material as the differently oriented single-crystal crystallites deform heterogeneously. This is further complicated by the localized residual stresses associated with the blockage of the glide of dislocations within the crystallites due to impurity inclusions, particularly in dispersion and precipitation hardened alloys (Lee, 1985).

A general formulation of the evolution equations for back stress can be expressed in terms of form-invariant tensor functions, the constants involved being determined by an experimental program of measuring the stress response to prescribed strain histories or vice versa. Such tests would involve a generalization of both the Prager-Ziegler strain-rate term and the rotation influence. The generalized Prager-Ziegler law proposed by Fardshisheh and Onat (1974), expressed as

$$\dot{\alpha}=\mathrm{h}(\alpha,\ \mathrm{D}^{\mathrm{p}})+\mathrm{W}\alpha-\alpha\mathrm{W} \tag{1}$$

is equivalent to using the Jaumann derivative

$$\hat{\alpha}=\mathrm{h}(\alpha,\ \mathrm{D}^{\mathrm{p}}) \tag{2}$$

where h can be represented in terms of certain basic functions (Agah-Tehrani, 1987) such that

$$\begin{aligned}\mathrm{h}(\alpha,\ \mathrm{D}^{\mathrm{p}})&=\eta_1\mathrm{D}^{\mathrm{p}}+\eta_2\dot{\bar{\varepsilon}}^{\mathrm{p}}\alpha+\eta_3\dot{\bar{\varepsilon}}^{\mathrm{p}}\left(\alpha^2-\frac{1}{3}\mathrm{tr}(\alpha^2)\mathrm{I}\right)\\&+\eta_4\left(\alpha\mathrm{D}^{\mathrm{p}}+\mathrm{D}^{\mathrm{p}}\alpha-\frac{2}{3}\mathrm{tr}(\alpha\mathrm{D}^{\mathrm{p}})\mathrm{I}\right)+\eta_5\left(\alpha^2\mathrm{D}^{\mathrm{p}}\right.\\&\left.+\mathrm{D}^{\mathrm{p}}\alpha^2-\frac{2}{3}\mathrm{tr}(\alpha^2\ \mathrm{D}^{\mathrm{p}})\mathrm{I}\right)+\bar{\mathrm{W}}\alpha-\alpha\bar{\mathrm{W}}\end{aligned} \tag{3}$$

where $\bar{\mathrm{W}}$ is an antisymmetric tensor function of $\dot{\bar{\varepsilon}}^{\mathrm{p}}=\sqrt{\frac{2}{3}\ \mathrm{D}^{\mathrm{p}}:\mathrm{D}^{\mathrm{p}}}$ the back stress α, the rate of plastic deformation D^{p}, and the rate of effective plastic strain. The relation between the rate of strain and the rate of deformation is defined by the form $\dot{\varepsilon}=\frac{\mathrm{d}\varepsilon}{\mathrm{dt}}=\mathrm{F}^{\mathrm{T}}\cdot\mathrm{D}\cdot\mathrm{F}$, where $\dot{\varepsilon}$ is the rate of strain, and F the deformation gradient. The back stress is a type of residual stress embedded in the deforming material, and the spin term in Eq. (1) expresses the contribution of the consequent rotation of the back stress to the material derivative with respect to fixed axes, in which W is the spin, the antisymmetric part of the velocity gradient. The form of the isotropic tensor function, h, is chosen in such a way that Eq. (3) will be rate independent, and therefore h must be linear in D^{p}. $\bar{\mathrm{W}}$ with linear terms in D^{p} has the form

$$\begin{aligned}\bar{\mathrm{W}}=&\phi_1(\alpha\mathrm{D}^{\mathrm{p}}-\mathrm{D}^{\mathrm{p}}\alpha)+\phi_2(\alpha^2\mathrm{D}^{\mathrm{p}}-\mathrm{D}^{\mathrm{p}}\alpha^2)\\&+\phi_3(\alpha\mathrm{D}^{\mathrm{p}}\alpha^2-\alpha^2\mathrm{D}^{\mathrm{p}}\alpha)\end{aligned} \tag{4}$$

The coefficients ϕ's and η's are functions of invar-

iant of α.

According to Agah-Tehrani *et al.* (1987), $\bar{W}$ is expressed in the simple form

$$\bar{W}=(\mathrm{tr}N)(\alpha D^p-D^p\alpha)-[N(\alpha D^p-D^p\alpha)+(\alpha D^p-D^p\alpha)N] \quad (5)$$

where $N=\phi_1 I-\phi_2\alpha+\phi_3[\frac{1}{2}\mathrm{tr}(\alpha^2)I-\alpha^2]$. Equation (5) reflects the fact that $\bar{W}$ can be obtained from the basic antisymmetric tensor $(\alpha D^p-D^p\alpha)$ and an isotropic tensor function of α. The first five terms in Eq. (3) which do not contain $\bar{W}$ are selected to incorporate the direct effect of the rate of strain and the second the influence of the rotation due to the straining of lines of material elements which carry the embedded back stress. Such rotations can have a significant spin effect independently of the spin W. Selection of the first term in Eq. (3) to express the direct effect of the rate of strain reduces (2) to

$$\hat{\alpha}=c\ D^p+\bar{W}\alpha-\alpha\bar{W} \quad (6)$$

where c is the classical Prager-Ziegler hardening modulus. All the first five terms are directly related with the loading strain, but it was assumed that the first term is dominant. Onat (1982) also proposed a similar form for the same purpose and it plays a similar role as the Prager-Ziegler kinematic hardening model. This is approximately verified with the experimental measurements as shown in part ‖ of this paper. Of course, the second, third and remainder terms may also be taken into account but this needs more careful experimental verification. Moreover, from a computational point of view, more terms will lead to more complicated manipulations. Therefore a simpler form will be preferred if the accuracy of the constitutive equation is not significantly decreased. Selecting the first term of Eq. (4) and non-dimensionalizing by the magnitude of the back stress, $\bar{W}$ will have the form (Lee and Agah-Tehrani, 1988)

$$\bar{W}=-\frac{\psi}{\sqrt{\alpha:\alpha}}[\alpha D^p-D^p\alpha] \quad (7)$$

ψ is a non-dimensional material dependent parameter which controls the contribution of the spin due to induced anisotropy. ψ will be nonzero if α and D^p have different principal directions. Only nonnegative values of ψ must be considered so that the spin of the eigen-triad of the embedded anisotropy is not larger than the average spin of the material particle. Introduction of the above expression for $\bar{W}$ has removed the anomaly arising from the choice of terms added to preserve objectivity in finite deformation analysis, such as the oscillation of the shear stress with increasing shear strain during simple shearing of a rectangular block (Suh *et al.*, 1991).

3. Approach of Verifying the Applicability of Combined Isotropic-Kinematic Hardening

3.1 Circle-fit of the yield surface data measured from non-proportional straining

Helling *et al.* (1986) observed that the developing yield surface inflates in the loading direction while a flattening of the yield surface is taking place in the opposite direction. Figure 1

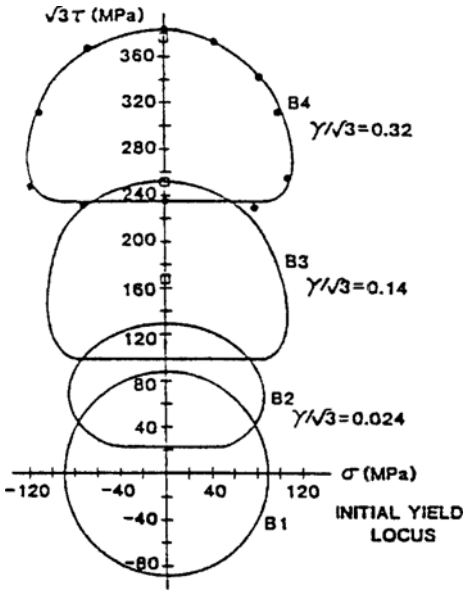

Fig. 1 Measured yield loci of 70 : 30 brass after shear prestress. (B1) : No prestress. (B2) : $\sqrt{3}\tau=167$MPa, $\frac{\gamma}{\sqrt{3}}=0.024$. (B3) : $\sqrt{3}\tau=252$MPa, $\frac{\gamma}{\sqrt{3}}=0.14$. (B4) : $\sqrt{3}\tau=378$MPa, $\frac{\gamma}{\sqrt{3}}=0.32$. $\sqrt{3}\times10^{-6}$ strain offset yield definition. From Helling *et al.* (Helling *et al.*, 1986).

from Helling *et al.* (1986) shows the evolving yield loci in the axial-generalized shear stress plane during monotonic shearing of a thin tube in torsion. The initial yield locus is well represented by the von Mises circle. As the shear strain increases, the protuberant nose, which can be fitted with the circle, progresses forward in the direction of increasing shear strain with a flattening of the opposite side of the yield surface. A similar result has been also observed by Cheng and Krempl (1991) in their tensile straining of an Al/Mg alloy at room temperature. They used thin-walled tubular specimens made of an Al/Mg alloy and conducted tests with a servohydraulic, computer controlled, MTS axial-torsion testing machine. The stress response was obtained for non-proportional strain paths under simultaneous axial and torsional straining. Figure 2 includes the proposed strain path in which a regular-polygonal strain path is followed by a square path. At certain predetermined points as shown in Fig. 2, a series of strain increment probes was introduced to determine the yield locus and consequently ascertain the path dependent anisotropy due to non-proportional loading. The path between the probing points corresponds to a sum of increments of strain several times the yield-point strain. Since one specimen is used to complete the whole strain path, in order to obtain a consistent evolution of stress response, a small offset strain of 10^{-4} was used to determine the yield locus so that appreciable hardening should be avoided during the yield stress probing. Details of the testing equipment and procedures have been described in Cheng and Krempl (1991).

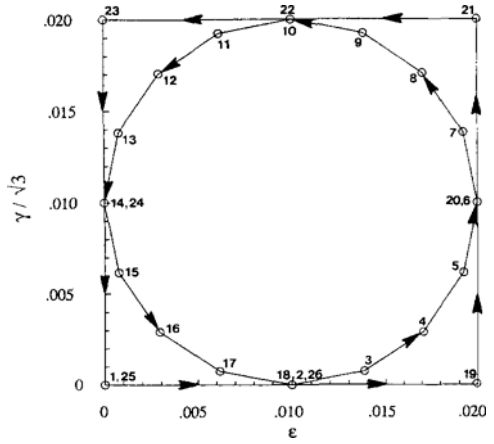

Fig. 2 Strain path for tension-torsion test of a thin-walled tube. After 1% of axial prestrain, a combination of axial(ε) and generalized shear($\frac{\gamma}{\sqrt{3}}$) strains are applied for polygonal followed by a square path. From Cheng and Krempl (Cheng and Krempl, 1991).

In this work, the evoluting yield surface was to be fitted with a circle especially on the nose geometry in order to examine whether the von Mises base combined isotropic-kinematic hardening can be applied to predict non-proportional straining problems. The experimental yield loci to be fitted were provided by Cheng and Krempl (1991).

3.2 Measure of the applicability through FEM prediction

In most metal-forming processes such as rolling or drawing, commonly a dimension in a narrow range of orientations, longitudinal or lateral, is being stretched or compressed throughout the plastic deformation and thus drastic changes of strain vector are not likely to occur. Of course, marked changes can be generated by the onset of instabilities and localization of the strain.

The validity of the application of combined isotropic-kinematic hardening requires that the

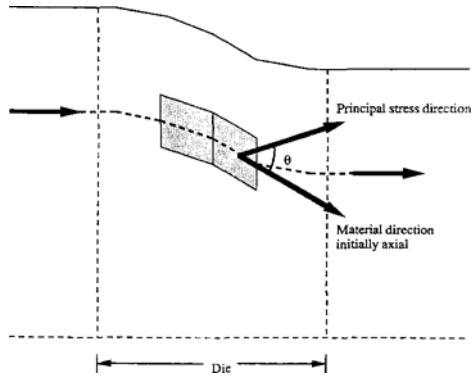

Fig. 3 Schematic of angle variation between the principal stress direction and the material direction, initially axial, inside the die during steady state axisymmetric extrusion. Upper half was shown because of symmetry.

stress point traverse a restricted area of the yield locus. This is achieved if the orientation of the principal stress does not deviate widely from the directions of the material elements in the body which have carried those stress components. This procedure is demonstrated by the finite element analysis of axisymmetric extrusion of a rod through a frictionless die. Lines directed axially in the billet again become axial in the extrudate, and their direction inside the die are given by the orientation of the corresponding edges of the sequentially updated Lagrangian finite elements, see Fig. 3.

4. Results and Discussion

4.1 Circle-fit to experimental yield data

The yield loci probed along the strain path depicted in Fig. 2 were numerically fitted by circles. The measurement of yield surfaces in axial -generalized shear stress space generate yield loci which exhibit a rounded nose in the direction of straining and are flattened in the rear as the literature indicates. The compatibility of the circle, which corresponds to combined isotropic -kinematic hardening, was assessed by a circle -fitting program which was developed to compute the circle through the nose of the yield surface using a least-squares fit. The program computes the center and radius of a circle from the scattered data. The sum of the errors corresponding to each data set is

$$\sum_{i=0}^{m} E_i = \sum_{i=0}^{m} [(x_i - a)^2 + (y_i - b)^2 - RD^2] \quad (8)$$

where (a, b) and RD are the center and radius of the fitted circle, respectively. The integer m indicates the selected number of points used. Now it is necessary to minimize

$$\Pi = \sum_{i=0}^{m} E_i^2 = \sum_{i=0}^{m} [(x_i - a)^2 + (y_i - b)^2 - RD^2]^2 \quad (9)$$

The multivariable Newton-Rhapson method (See, Press *et al*. 1986 ; Yakowitz and Szidarovszky, 1986, for example) was used to optimize Π. This method requires the evaluation of the first and second partial derivatives of Π. The initial

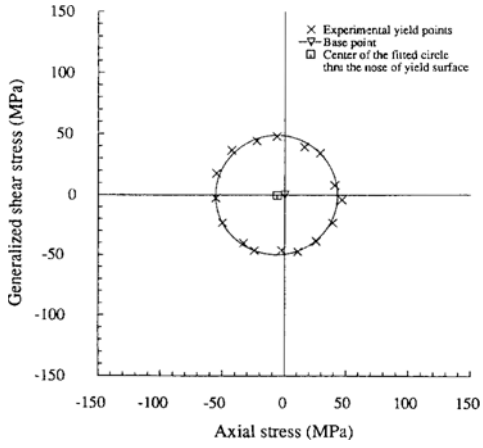

Fig. 4 Experimental initial yield locus with a numerically-fitted circle. This corresponds to the probing station 1 in Fig. 2.

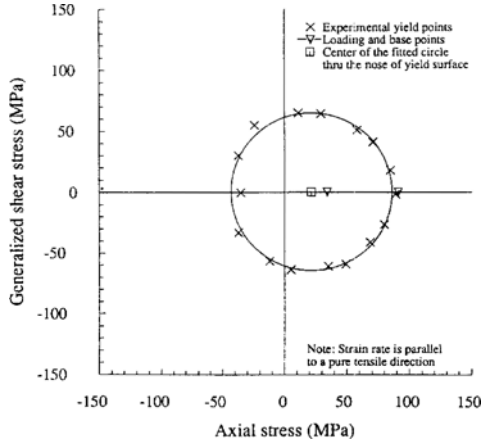

Fig. 5 Experimental initial yield locus with a numerically-fitted circle at station 2, 1% tensile prestrain.

yield locus was fitted and is shown in Fig. 4, which indicates that the locus can be accurately described by the von Mises yield criterion. Figure 5 shows the fitted circle for the yield locus for prestraining of 1% in the direction of pure tension (station 2 in the prescribed strain path, Fig. 2). The fitting was based on a ten component data set over the nose geometry of the yield locus involving a five data set on each side of the axis of the prestraining direction. Yield loci with circle-fit at Stations 6, 10, 14, 18 are shown in Figs. 6~9. In all cases except the rear part of yield locus (rear in the sense of opposite the direction of strain-

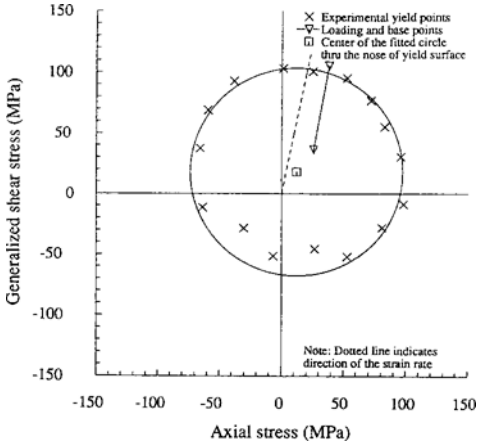

Fig. 6 Experimental initial yield locus with a numerically-fitted circle at station 6.

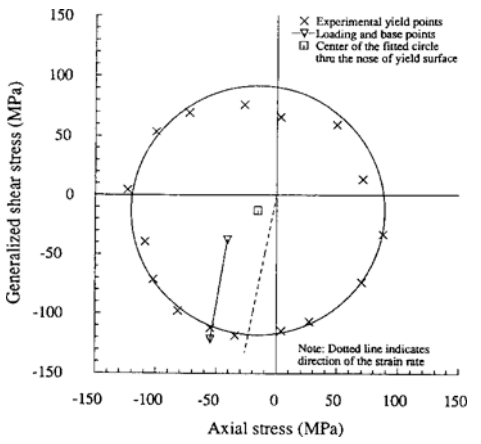

Fig. 8 Experimental initial yield locus with a numerically-fitted circle at station 14.

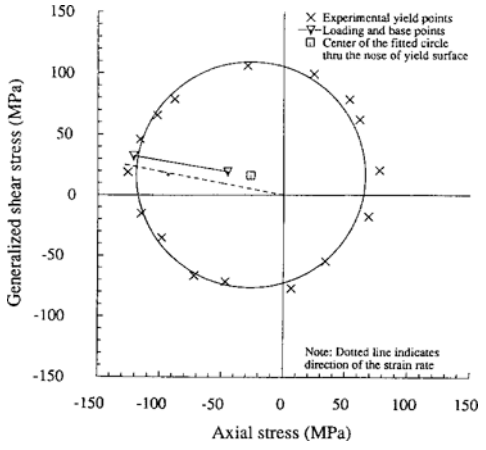

Fig. 7 Experimental initial yield locus with a numerically-fitted circle at station 10.

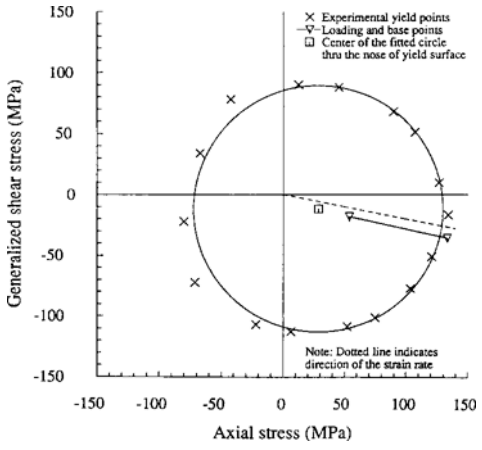

Fig. 9 Experimental initial yield locus with a numerically-fitted circle at station 18.

ing), fitted circles which correspond to combined isotropic-kinematic hardening show quite good agreement with the given experimental yield loci. This indicates that if the direction of the deformation is not totally reversed and the loading stress remains on the circular nose geometry, the prediction of stress response from arbitrary deformations will be very accurate. It is noted that the validity of combined isotropic-kinematic hardening is well demonstrated through this work.

Now that we have verified that circle is a reasonable fit to the von Mises yield surface, it would be very informative if the center and radius of circle are represented as a function of the back stress so that it can be determined with experimental measurements. Defining the back stress in stress space can differ according to the measure adopted. It is important to recognize that the center of yield locus in the axial stress-generalized shear stress space cannot be identified directly as the components of the back stress because of its deviatoric nature. The correlation formulae expressing the von Mises yield circle in the axial stress-generalized shear space have been derived in terms of the stress and the back stress as the following. In the tension-torsion test of a thin walled tube, the Cauchy stress components are

$$\sigma=\begin{pmatrix}\sigma & \tau & 0\\ \tau & 0 & 0\\ 0 & 0 & 0\end{pmatrix} \tag{10}$$

and the back stress components are

$$\alpha=\begin{pmatrix}\alpha_{zz} & \alpha_{z\phi} & 0\\ \alpha_{z\phi} & \alpha_{\phi\phi} & 0\\ 0 & 0 & -(\alpha_{zz}+\alpha_{\phi\phi})\end{pmatrix} \tag{11}$$

since α is a deviatoric stress. Combined isotropic-kinematic hardening gives the yield condition

$$(\sigma'-\alpha)\ :\ (\sigma'-\alpha)=\frac{2}{3}\bar{\sigma}^2=(\sigma'_{ij}-\alpha_{ij})\ :\ (\sigma'_{ij}-\alpha_{ij}) \tag{12}$$

which is a hypersphere. Here, $\bar{\sigma}$ is the effective stress. In tension-torsion testing, the yield condition is reduced to

$$(\frac{2}{3}\sigma-\sigma_{zz})^2+(-\frac{1}{3}\sigma-\alpha_{\phi\phi})^2+(-\frac{1}{3}\sigma+\alpha_{zz}+\alpha_{\phi\phi})^2+2(\tau-\alpha_{z\phi})^2=\frac{2}{3}\bar{\sigma}^2 \tag{13}$$

Rearranging, this can be expressed as a circle in the axial stress-generalized shear stress ($\sigma-\sqrt{3}\tau$) space :

$$(\sigma-\frac{3}{2}\alpha_{zz})^2+(\sqrt{3}\tau-\sqrt{3}\alpha_{z\phi})^2=\bar{\sigma}^2-3(\frac{1}{2}\alpha_{zz}+\alpha_{\phi\phi})^2 \tag{14}$$

Therefore, the center of the yield locus in terms of the back stress components in the axial stress-generalized shear stress ($\sigma-\sqrt{3}\tau$) space is represented with $(\frac{3}{2}\alpha_{zz},\ \sqrt{3}\alpha_{z\phi})$. If the yield locus is measured and fitted as a circle, the center is determined and thus α_{zz} and $\alpha_{z\phi}$ are obtained. Once these have been established, the basic information is available to assess the terms needed in the evolution equation for the back stress α, the most general form of which is given by Eq. (3). To do so, extensive and elaborated experiments are required. In this work, a parametric evaluation of Eq. (6), which is a simpler form obtained by taking the first and the rotational terms from Eq. (3), was carried out and presented separately in part Ⅱ.

4.2 Applicability of Combined Isotropic-Kinematic Hardening in an Extrusion Process

The finite element code used for the present analysis is IFDEPSA (Incremental Finite Deformation Elastic-Plastic Stress Analyzer) (Suh *et al.*, 1991). IFDEPSA uses the updated Lagrangian method for solving large deformation elastic-plastic problems. Because of the axial symmetry, only half of the workpiece was considered. This symmetry condition requires that there will be zero shear stress and zero normal velocity along the axis. The driving force was applied by a rigid frictionless piston with a prescribed velocity. The billet was assumed to be snugly fitted into the die such that there were no initial stresses. The calculations were carried out for a 25% reduction in the area. The length of the die was $1.2r_o$, with r_o the initial radius of the billet. The die contour was assumed to be a smooth curve represented by a 5th-order polynomial with zero slope and curvature at both ends. Material for this computation was 24S-T aluminum, whose initial and saturation yield stress are respectively 269 MPa and 517 MPa. Young's modulus was 68,950 MPa and Poisson's ratio was 0.33. The mesh consisted of 58 elements along the axial direction and 11 elements along the radial direction, with progressively narrower elements close to the outer surface of the billet. The finite element mesh is shown in Fig. 10. For the analysis, a total of 580 incremental steps were utilized such that 40 increments were needed for each column of elements to advance 3 element sizes in the axial direction. A detailed finite-element formulation for running the present analysis is described in Suh *et al.* (1991).

The stresses were obtained with combined isotropic-kinematic hardening ($\beta=0.5$) with an appropriate contribution of spin associated with induced anisotropy ($\psi=-4.0$) which was shown to generate qualitatively close agreement with the experimental stress pattern, in Suh *et al.* (1991). β is a material-dependent hardening parameter such that isotropic hardening corresponds to $\beta=1$, and kinematic hardening to $\beta=0$. The computation was carried out on the centroid of each rectangular element. Figure 11 shows the statisti-

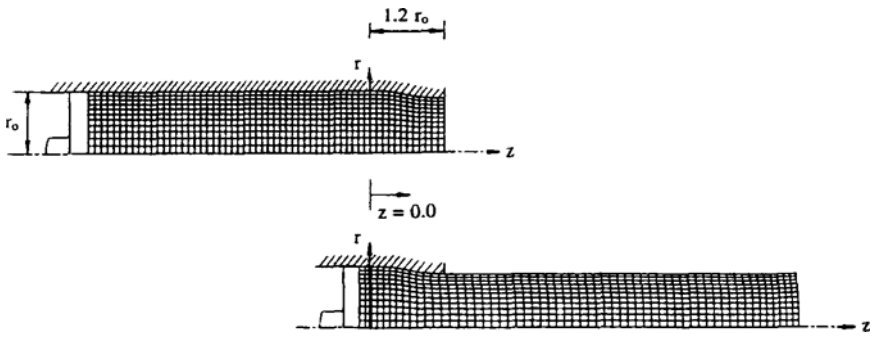

Fig. 10 Undeformed and deformed mesh configurations. The deformed mesh configuration was obtained after the piston moved forward by 580 incremental steps with combined isotropic-kinematic hardening ($\beta=0.5$, $\psi=-4.0$). Due to symmetry, only one half of the billet is illustrated.

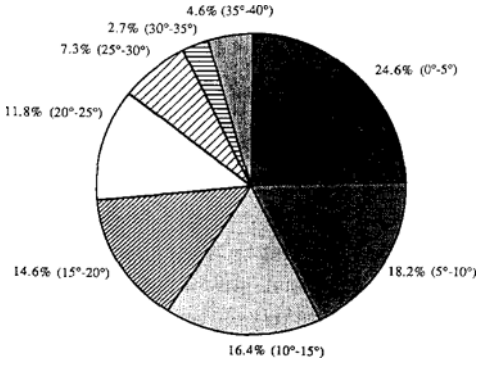

Fig. 11 Statistical distribution of angle variation computed under the scheme shown in Fig. 3.

cal distribution of the variation of the angle between the principal stress and material directions inside the die, where most of the plastic deformation is taking place. Out of 132 elements inside the die, almost 60% of the angles are less than 15° and even the largest is less than 40°. Experimental yield surfaces show that, for such a mild change of the stress tensor, the stress point will move along the yield locus exhibiting nearly uniform curvature. It is conjectured from computational results that even with larger still practical reduction ratios, the loading stress point will reside on the nose circle geometry of the yield surface. This allows us to use the combined isotropic-kinematic hardening model for convenient computations in the stress analysis of extrusions of appropriate reduction ratios, or possibly of various metal forming processes.

5. Conclusions

The applicability of combined isotropic -kinematic hardening theory was verified by showing its conformity with experimental yield loci, and an FEM calculation of an extrusion process was carried out as a measure of checking the applicability of the combined isotropic -kinematic hardening model to the general straining problem like extrusion process. The results from this work are as follows :

(1) A computer program that fits a circle through the nose of the yield locus in generalized stress space has been developed to evaluate the applicability of combined hardening to the experimental yield surfaces obtained from the nonproportionally prescribed strain path. The center and radius of the circle, which correspond to the kinematic and isotropic components of hardening, were obtained by the least-squares fitting method. It was found that noses of experimental yield loci that have gone through a nonproportional straining path are well represented by a fitted circle. This indicates that restricted traverses of the stress point over the nose of the yield surface, exhibiting nearly uniform curvature, simplifiy the selection of the reliable constitutive relation.

(2) The general isotropic-kinematic hardening yield condition which expresses a hypersphere in stress space was represented in two dimension with center and radius in tension-torsion space in terms of the back stress. This will contribute to

establishing a new hardening model based on experimental measurements, since the evolution equation of back stress can be assessed in three dimensions from the experimental yield loci. The measurement set up has to be carefully designed so that unwanted factors such as material instability or measuring error are avoided. This will be left as future research.

(3) A means of checking the applicability of combined isotropic-kinematic hardening in analyzing the total stress history was demonstrated by simulating an extrusion process using the finite -element method. Numerical evaluations of the steady-state stress distribution generated during axisymmetric extrusion revealed that the variation of the angle between the corresponding principal stress and material directions in the plastic deformation region is small enough to ensure that the stress point will remain in the neighborhood of the nose of the yield surface, and that the stress analysis can thus be based on combined isotropic -kinematic hardening.

The combined isotropic-kinematic hardening model, however, has some limitations in stress analyses involving instability, localization or cyclic straining where the change of the stress vector could be drastic. To analyze those problems, a hardening model associated with shape changes of the yield surface needs to be developed.

Acknowledgements

The author would like to thank Prof. E. Krempl of Rensselaer Polytechnic Institute and Dr. S. Cheng of Concurrent Technologies Corporation for providing valuable experimental data. The generous advice of Dr. E. H. Lee, Emeritus Professor at both Rensselaer Polytechnic Institute and Stanford University, is gratefully acknowledged. Partial support of the 1997 Academic Research Fund from Hannam University is gratefully acknowledged.

References

Agah-Tehrani, A., Lee, E. H., Mallett, R. L. and Onat, E. T., 1987, "The Theory of Elastic-Plastic Deformation at Finite Strain with Induced Anisotropy Modeled as Combined Isotropic-Kinematic Hardening," *J. Mech. Phys. Solids*, Vol. 35, pp. 519~539.

Cheng, S. and Krempl, E., 1991, "Experimental Determination of Strain-Induced Anisotropy During Nonproportional Straining of an Al/Mg Alloy at Room Temperature," *Int. J. Plasticity*, Vol. 7, pp. 827~846.

Dafalias, Y. F., 1983, "Corotational Rates for Kinematic Hardening at Large Plastic Deformations," *J. Appl. Mech.*, Vol. 50, pp. 561~565.

Dafalias, Y. F., 1985a, "The Plastic Spin," *J. Appl. Mech.*, Vol. 52, pp. 865~871.

Dafalias, Y. F., 1985b, "A Missing Link in the Macroscopic Constitutive Formulation of Large Plastic Deformation," in Sawczuk, A. and Bianchi, G. (eds.), *Plasticity Today-Modelling, Methods and Applications*, Elsevier Applied Science Publishers, pp. 135~152

Fardshisheh, F. and Onat, E. T., 1974, "Representation of Elastoplastic Behavior by means of State Variables," in Sawczuk, A. (ed.), *Problems in Plasticity*, Noordhoff International Publishing, pp. 89~115.

Gupta, N. K. and Meyers, A., 1986, "Description of Initial and Subsequent Yield Surfaces," *Z. Angew. Math. Mechanik*, Vol 66, pp. 435~439.

Gupta, N. K. and Meyers, A., 1992, "Consideration of Translated Stress Deviators in Describing Yield Surfaces," *Int. J. Plasticity*, Vol. 8, pp. 729 ~740.

Helling, D. E., Miller, A. K. and Stout, M. G., 1986, "An Experimental Investigation of Yield Loci of 1100-0 Aluminium, 70 : 30 Brass, and an Overaged 2024 Aluminium Alloy after Various Prestrains," *J. Engg. Matls and Tech.*, Vol. 108, pp. 313~320.

Helling, D. E., Miller, A. K., 1987, "The Incorporation of Yield Surface Distortion into a Unified Constitutive Model, Part I," *Acta Mechanica*, Vol. 69, pp. 9~23.

Kuroda, M., 1995, "Plastic Spin Associated with a Corner Theory of Plasticity," *Int. J. Plasticity*, Vol. 11, pp. 547~570.

Kurtyka, T and Zyczkowski, M., 1985, "A

Geometric Description of Distortional Plastic Hardening of Deviatoric Materials," *Arch. Mech.*, Vol. 37, pp. 383~395.

Kurtyka, T and Zyczkowski, M., 1996, "Evolution Equation for Distortional Plastic Hardening," *Int. J. Plasticity*, Vol. 12, pp. 191~213.

Lee, E. H., 1985, "Interaction between Physical Mechanisms and the Structure of Continuum Theories," in Gittus, J., Zarka, J. and Nemat-Nasser, S. (eds.), *Large Deformations of Solids-Physical Basis and Mathematical Modelling*, Elsevier Applied Science, pp. 143~161.

Lee, E. H. and Agah-Tehrani, A., 1988, "The Structure of Constitutive Equations for Finite Deformation of Elastic-Plastic Materials involving Strain-Induced Anisotropy with Applications," *Int. J. Num. Meth. Eng.*, Vol. 25, pp. 133~146.

Loret, B., 1983, "On the Effects of Plastic Rotation in the Finite Deformation of Anisotropic Elastoplastic Materials," *Mech. Mat.*, Vol. 2, pp. 287~304.

Mandel, J., 1971, *Plasticit Classique et Viscoplasticit, Courses and Lectures, No. 97*, International Center for Mechanical Sciences, Udine, Springer-Verlag.

Mazilu, P. and Meyers, A., 1985, "Yield Surface Description of Isotropic Materials After Cold Predtrain," *Ing. Archiv*, Vol. 55, pp. 213~220.

Nagtegaal, J. C. and de Jong, J. E., 1982, "Some Aspects of Non-Isotropic Work Hardening in Finite Strain Plasticity," in Lee, E. H. and Mallett, R. L. (eds.), *Plasticity of Metals at Finite Strain : Theory, Experiment and Computation*, Division of Applied Mechanics, Stanford University and Department of Mechanical Engineering, Aeronautical Engineering and Mechanics, Rensselaer Polytechnic Institute, pp. 65~102.

Ning, J. and Aifantis, E. C., 1997, "Anisotropic Yield and Plastic Flow of Polycrystalline Solids," *Int. J. Plasticity*, Vol. 12, pp. 1221~1240.

Onat, E. T., 1982, "Representation of Inelastic Behavior in the Presence of Anisotropy and of Finite Deformation," in Wilshire, B. and Owen, D. R. J. (eds.), *Recent Advances in Creep and Fracture of Engineering Materials and Structures*, Pineridge Press, pp. 231~264.

Paulun, J. E. and Pecherski, R. B., 1985, "Study of Corrotational for Kinematic Hardening in Finite Deformation Plasticity," *Arch. Mech.*, Vol. 37, pp. 661~677.

Paulun, J. E. and Pecherski, R. B., 1987, "On the Application of the Plastic Spin Concept for the Description of Anisotropic Hardening in Finite Deformation Plasticity," *Int. J. Plasticity*, Vol. 3, pp. 303~314.

Suh, Y. S., Agah-Tehrani, A. and Chung, K., 1991, "Stress Analysis of Axisymmetric Extrusion in the Presence of Induced Anisotropy Modeled as Combined Isotropic-Kinematic Hardening," *Comp. Meth. Appl. Mech. Engng.*, Vol. 93, pp. 127~150.

Van Der Giessen, E., Wu, P. D., and Neale, K. W., 1992, "On the effect of Plastic Spin on Large Strain Elastic-Plastic Torsion of Solid Bars," *Int. J. Plasticity*, Vol. 8, pp. 773~801.

Voyiadjis, G. Z. and Foroozesh, M., 1990, "Anisotropic Distortional Yield Model," *J. Appl. Mech.*, Vol. 57, pp. 537~547.

Zbib, H. M. and Aifantis, E. C., 1987, "Constitutive Equations for Large Material Rotations," in Desai, C. S. et al. (eds.), *Constitutive Laws for Engineering Materials : Theory and Applications*, Elsevier Science Publishing Co., Inc., pp. 1411~1418.

Zbib, H. M. and Aifantis, E. C., 1988a, "On the Concept of Relative and Plastic Spins and its Implications to Large Deformation Theories Part Ⅰ : Hypoelasticity and Vertex-Type Plasticity," *Acta Mech.*, Vol. 75, pp. 15~33.

Zbib, H. M. and Aifantis, E. C., 1988b, "On the Concept of Relative and Plastic Spins and its Implications to Large Deformation Theories Part Ⅱ : Anisotropic Hardening Plasticity," *Acta Mech.*, Vol. 75, pp. 35~56.